Study of Light Transport in Multilayered Turbid Media

A thesis submitted towards partial fulfillment of

BS-MS Dual Degree Programme

by

Dinesh Kumar

20091081

Under the guidance of

Dr. Ramasubramaniam Rajagopal

Senior Research Scientist

Unilever R &D Bangalore

64, Main Road, Bangalore-560066

INDIAN INSTITUE OF SCIENCE EDUCATION AND RESEARCH

PUNE

CERTIFICATE

This is to certify that this dissertation entitled **Study of light transport in multilayered turbid media** towards the partial fulfillment of the BS-MS dual degree program at the Indian Institute of Science Education and Research (IISER), Pune represents original research carried out by **Mr. Dinesh Kumar,** at **Unilever R&D Bangalore** under the supervision of **Dr. Ramasubramaniam Rajagopal, Unilever R&D Bangalore.**

Dinesh Kumar

20091081

IISER, Pune

Dr. Ramasubramaniam Rajagopal

Senior Research Scientist

Unilever R&D Bangalore

Acknowledgements

First of all I would like to thank Hindustan Unilever Research Centre for giving me such a great opportunity of exploring research areas and for giving me an opportunity to do this project.

I am grateful to my thesis advisor Dr. Ramasubramaniam Rajagopal, for mentoring and giving valuable guidelines. It would have been impossible to achieve this goal without his constant support, encouragement and also his joking jabs at my incompetence. Dr Ram, It has been an honor to work with you.

I would also like to thank Mr. Arindam Roy my co-guide, for helping me in the project and providing important suggestions.

Last but not the least I am extremely thankful to all the lab mates and all those who directly and indirectly helped me in this thesis.

Abstract

Many materials observed in nature exhibit multilayer optical structures. Few examples include skin of humans, epithelial cells, leaf in plants etc. The optical properties of these materials are of great interest to scientists for variety of reasons including disease diagnosis, chlorophyll estimation etc. However most of these materials exhibit strong scattering and measurement of absorption properties of these materials becomes difficult since it is not possible to decouple absorption from scattering using standard absorption spectroscopy techniques. Various authors have tried to use diffuse optical spectroscopy to address this. However these measurements involve computer intensive calculations to obtain optical parameters from the diffuse optical spectra. Kubelka-Munk (K-M) theory is a phenomenological light transport theory that provides analytical expressions for reflectance and transmittance of diffusive substrates. Many authors have derived relations between coefficients of K-M theory and that of the more fundamental radiative transfer equations (RTE). In this thesis, we have modified an empirical model developed earlier by Roy et al to relate the K-M and RTE coefficients and improved its accuracy.

We have validated the feasibility of using these empirical relations to decouple the absorption and scattering properties of a turbid medium. We find that in presence of absorption, the scattering properties of a scattering material decreases. We have developed an empirical equation to obtain the reduced scattering coefficient of the pure scattering material from the scattering properties of the same material in the presence of absorption which can predict the reduced scattering coefficient very accurately.

We have built a double layer optical model using the K-M theory. In order to validate the model we developed optical phantoms using a mix of PDMS and commercially available iron oxide particles. Using the empirical relations and the double layer model we can extract the optical properties of the double layer optical phantom system within an error of 10% establishing the feasibility that this model can be used to study the optical properties real systems such as skin tissues and plant leafs.

List of Figures

Figure 1.1. Schematic representation of light transport in a turbid medium modeled using the Kubelka-Munk (K-M) theory. I and J depict diffuse fluxes traveling in the forward and backward directions, respectively. S and K are the K-M backscattering and absorption coefficients of the medium respectively. Sample thickness is denoted by t.

Figure 2.1. Schematic diagram of the method used to obtain empirical relations between radiative transport coefficients and the Kubelka-Munk coefficients. From the measured total reflectance (R) and transmittance (T), the K-M coefficients were calculated and related. This method was borrowed from the work of Roy et al.

Figure 2.2. Measurement configuration used to measure (a) Total reflectance and (b) Total transmittance.

Figure 2.3. K-M scattering coefficient S as a function of reduced scattering coefficient ms' of the polystyrene microspheres. Each cluster of points corresponds to different concentration of polystyrene spheres and different points in a cluster correspond to different wavelengths. The solid line is the best linear fit obtained.

Figure 2.4. The actual (circles) and extracted (solid line) values of (a) absorption coefficient of the dye and (b) linear fit between actual and extracted absorption coefficient of the dye showing less than 2% variation, (c) reduced scattering coefficient of pure polystyrene spheres (solid line) and polystyrene spheres in the presence of dye (circles).

Figure 3.1. The absorption coefficient of a polystyrene spheres and dye mix extracted using the empirical equation 2.5 for three different dye concentrations. (b). the reduced scattering coefficients of the pure polystyrene sand polystyrene-dye mix with three different dye concentrations extracted using equation 2.5.

Figure 3.2. The difference between the reduced scattering coefficient of pure polystyrene spheres (solid line) and the reduced scattering coefficient obtained using the equation 2.1 (markers) was minimized by varying the parameter *a*. Best fit was obtained for a =1.1

Figure 3.3. The reduced scattering coefficient of polystyrene spheres (diamonds) was extracted from the reduced scattering coefficient of the polystyrene and dye mix using equation 3.3. The reduced scattering coefficient of pure polystyrene spheres is also shown (solid line). This data is same as the data shown in figure 2.3 c.

Figure 4.1. Images of optical phantoms used in the multi-layer model study

Figure 4.2. (a) Reflectance and (b) transmittance values of the two individual tissue phantoms

Figure 4.3. The specific absorption and specific reduced scattering coefficients of the iron oxide used in the optical phantoms, calculated using the empirical relation shown in equation 2.5

CONTENTS

1.INTRODUCTION: LIGHT TRANSPORT IN TURBID MEDIUM 8

1.1 Absorption 8

1.1.1 Laws of absorption 9

1.1.2 Lambert's law 9

1.1.3 Beer's law 10

1.1.4 Limitations of Beer-Lambert law 10

1.2 Light Scattering 11

1.2.1 Single and Multiple Scattering 11

1.2.2 Rayleigh scattering theory 12

1.2.3 Mie scattering theory 11

1.3 Absorption in presence of scattering 12

1.3.1 Radiative transfer equation 13

1.3.2 RTE in diffuse media 13

1.3.3 Kubelka-Munk Theory 14

2.RELATION BETWEEN KUBELKA-MUNK AND RADIATIVE TRANSFER EQUATION COEFFICIENTS 17

2.1 Material and Methods 19

2.1.1 Sample Preparation 19

2.1.2 Spectral Measurements 20

2.1.3 Calculation of absorption and reduced scattering coefficients 21

2.2 Results and Discussion 21

2.2.1 Derivation of Empirical Relation between K-M and RTE coefficients 21

2.2.2 Validation of the empirical equation 24

3. EMPIRICAL RELATION BETWEEN REDUCED SCATTERING COEFFICIETNS IN THE ABSENCE AND PRESENCE OF ABSORBING MEDIUM 25

3.1 Materials and Methods 25

3.2 Results 25
3.3 Development of empirical relation between reducing scattering coefficients in the presence and absence of absorbing medium 27
4. DEVELOPMENT OF A DOUBLE LAYER TURBID MEDIA MODEL 30
4.1 Materials and Methods 30
4.1.1 Theory 30
4.1.2 Optical Phantoms 31
4.2 Results and Discussion 32
5. CONCLUSION 36
REFERENCES 37

Chapter 1

INTRODUCTION: LIGHT TRANSPORT IN TURBID MEDIUM

The interaction between light and matter determines the appearance of everything around us, from the color of the sky, the way we look etc. Generally light interacts with any medium in multiple ways such as reflection, absorption, scattering, etc. In this chapter we will introduce how light interacts differently with matter, how these interactions dictate light transport through materials and theoretical description of these interaction and transport.

In section 1.1 we describe the phenomena of light absorption, Beer's & Lambert law and their limitation. In section 1.2 we discuss basic theories behind light scattering, Mie theory of scattering, Rayleigh approximation and the parameters used to define it. The discussion will be limited to elastic scattering, in which there is no loss in energy of the scattered light. Section 1.3 describes the case of absorption in the presence of scattering and the theories that are used to understand the Radiative Transfer equation & Kubelka-Munk Theory.

1.1 Absorption

When light enters a medium, the atom and molecules present in the medium absorb the photons and will move into higher energy excited states. These excited atoms or molecules can relax back to the ground state either through a radiative process or non radiative process. If these molecules relax back through emission of a photon with same energy as incident light photon, the process is elastic and no energy is lost. However, in many scenarios, the atoms and molecules collide with the neighboring atoms losing energy in the form heat or they lose energy through small energy vibrational motion. While light energy is absorbed by the molecule, it is converted into heat or other form of energy and hence the light is attenuated. This process in which the intensity of a beam of light is attenuated in passing through a material medium by conversion of the energy of the radiation to an equivalent amount of other forms of energy is called absorption.

A perfectly transparent medium permits the passage of a beam of radiation without any change in intensity other than that caused by the spread or convergence of the beam and the total radiant energy is emergent from such a medium equals that which entered it, where as the emergent

energy from an absorbing medium is less than that which enters, and, in the case of highly opaque media, is reduced, practically to zero.

No known medium is opaque to all wavelengths of the electromagnetic spectrum; similarly no material media is transparent to the whole electromagnetic spectrum. A medium which absorbs a relatively wide range of wavelengths is said to exhibit general absorption for those particular region, while a medium which absorbs only restricted wavelengths regions of no great range exhibits selective absorption for those particular spectral regions.

1.1.1 Laws of absorption

The capacity of a medium to absorb radiation depends on a number of factors, mainly the electronic and nuclear constitution of the atoms and molecules of the medium, the wavelength of the radiation, and the thickness of the absorbing layer, temperature and the concentration of the absorbing agent. Absorption is generally described by two theories namely Lambert's law and Beer's law.

1.1.2 Lambert's law

Lambert's law expresses the effect of the thickness of the absorbing medium on the absorption. If I is the intensity to which a monochromatic parallel beam is attenuated after traversing a thickness d of the medium, and I_0 is the intensity of the beam at the surface of incidence, the variation of intensity throughout the medium is expressed as

$$I = I_0 \exp(-\mu_a d) \tag{1.1}$$

Where μ_a is a constant for the medium called the *absorption coefficient*. This exponential relation can be expressed in an equivalent logarithmic form

$$\log_{10}(I_O/I) = kd \tag{1.2}$$

Where $k = (\mu_a/2.303)$ is called the extinction coefficient of the medium. The quantity $\log_{10}(I_O/I)$ is often called the *optical density*, or the *absorbance* of the medium. Equation (1.1) and (1.2) show that the absorption and extinction coefficients have the dimensions of reciprocal length.

1.1.3 Beer's law

This law refers to the effect of the concentration of the absorbing medium on the absorption. According to Beer's law, each individual molecule of the absorbing material absorbs the same fraction of the radiation incident upon it, no matter whether the molecules are closely packed in a concentrated solution or highly dispersed in a dilute solution. The relation between Intensity and concentration of the absorbing material at constant thickness is the exponential one, is same as the relation between the Intensity and thickness of the absorbing medium as expressed in Lambert's Law. So the effect of thickness d and concentration c on absorption of monochromatic radiation can therefore be combined in a single expression given in Equation (1.3).

$$I = I_0 \exp(-k' cd) \tag{1.3}$$

Where *k'* is a constant for a given absorbing substance .In logarithms, the relation becomes Equation (1.4).

$$\log_{10}(I_O/I) = (k'/2.303)cd = \varepsilon cd \tag{1.4}$$

The values of the constants *k'* and ε in Equations (1.3) and (1.4) depend on the units of concentration. If the concentration of the solute is expressed in moles per liter, the constant ε is called the molar extinction coefficient.

1.1.4 Limitations of Beer-Lambert law

The linear relationship between absorbance and concentration of an absorbing species is limited by chemical and instrumental factors. Causes of nonlinearity include:

- Scattering of lights due to particulates in the sample, as a result light doesn't travel in straight line.
- Stray light (Light may be from intended source but follow path other than intended).
- At very high concentrations, the molecules start interacting and the relation between absorbance and concentration becomes non-linear.

1.2 Light Scattering

A wide variety of real world-systems exhibit both absorption and scattering phenomena, in which light transport becomes randomized and doesn't travel in a straight line. Due to this randomization of light paths, quantification of absorption losses using Beer-Lambert's law Equation (1.3) is no longer possible. So to study such systems various scattering theories and models have been developed which works very well with absorption as well as scattering. It can be thought of as the deflection of a ray from a straight path, for example by irregularities in the propagation medium, particles, or in the interface between two media.

1.2.1 Single and Multiple Scattering

When radiation is only scattered by one localized scattering center called as single scattering and when scattering centers are grouped together known as multiple scattering. Single scattering can be treated as a random phenomenon while multiple scattering is more stochastic. In the investigated sample if the concentrations of particles are doubled and the scattered intensity also gets doubled and it is said that multiple scattering is absent and single scattering is important. Another criterion to differentiate between these is based on extinction. The intensity of a beam passing through the sample is reduced by extinction to $e^{-\tau}$ of its original value. Here τ is the optical depth of the sample along this line. If $\tau < 0.1$ single scattering prevails; If $0.1 < \tau < 0.3$ a correction for double scattering may be necessary, for $\tau > 0.3$ multiple scattering comes into the picture.

1.2.2 Rayleigh scattering theory

It is the elastic scattering of light by molecules and particular matter much smaller than the wavelength of the incident light. Rayleigh scattering intensity has a very strong dependence on the size of the particles (proportional to the sixth power of their diameter). It is inversely proportional to the wavelength of light, which means that the shorter wavelengths in visible white light (violet and blue) are scattered stronger than the longer wavelengths toward the red end of visible spectrum. This type of scattering is therefore responsible for the blue colour of the sky during the day, and orange colour during sunrise and sunset. The intensity (I) of the scattered radiation is given by

$$I = \frac{I_o 8\pi^4 N\alpha^2 (1+\cos^2\theta)}{\lambda^4 R^2} \tag{1.5}$$

Where I_O is the light intensity before the interaction with the particle, N is the number of scattering particles, R is the distance between the particle and the observer , θ is the scattering angle, λ the wavelength of the incident light and α is the polarizability . It can be seen from the above equation that Rayleigh scattering is strongly dependent upon the wavelength of the incident light, it dominates below 650 nm. Furthermore, the intensity of Rayleigh scattered radiation is identical in the forward and reverse directions.

The Rayleigh scattering breaks down when the particle size becomes larger than around 10% of the incident radiation. In the case of particles with dimensions greater than this, Mie's theory comes into the picture.

1.2.3 Mie scattering theory

It is a broad class of scattering of light by spherical particles of any diameter .The scattering intensity is generally not strongly dependent on the wavelength, but is sensitive to the particle size, Mie scattering intensity for large particles is proportional to the square of the particle diameter, means the greater the particle size, the more of the light is scattered in forward direction. Due to high dependence on the particle size, Mie theory (the physical solution of Mie scattering) is widely used in atmospheric science, particle sizing, cancer detection and screening, and metamaterial. Mie solutions are known only for well-defined spherical shaped and uniformly sized particles.

1.3 Absorption in presence of scattering

A wide variety of real-world systems exhibit both absorption and scattering phenomena. Due to scattering, light doesn't travel in a straight line and as a consequence, quantification of absorption losses using Beer-Lambert's law shown Equation (1.4) is no longer possible. To study such systems we need to look at other theories and models which work well with absorption and scattering simultaneously. One such theory is Radiative transfer equation (RTE).

1.3.1 Radiative transfer equation

Radiative transfer equation (RTE) treats light as a form of radiation energy and models how the energy flows and interacts with the media. Consider a small packet of light energy L, defined by its position r and its direction of propagation $\hat{s}$, called the spectral radiance which acts as the fundamental quantity in RTE. The radiance $L(r,\hat{s})$ can be lost either by absorption or scattering. But it also can be gained from the light scattered into its direction from other direction $\hat{s}'$.These two processes are captured by the radiative transfer equation

$$\hat{s}.\nabla L(r, \hat{s}') = -(\mu_a + \mu_s) L(r, \hat{s}) + (\mu_s/4\pi)\int p(\hat{s}, \hat{s}')d\Omega \quad (1.6)$$

Here the integral is over all solid angles and $d\Omega$ is the differential solid angle in the direction $\hat{s}$. μ_a, μ_s are the absorption and scattering coefficients of the media also known as the radiative transport coefficients. $p(\hat{s}, \hat{s}')$ is the scattering phase function and it is defined as the probability that photons travelling in the direction $\hat{s}$ are scattered Into the $\hat{s}$ direction [1.3-1.4]. The scattering phase function is normalized as $\int p(\hat{s}, \hat{s}')d\Omega$ over all angles.

RTE ignores wave amplitude and phases and hence cannot describe wave phenomena like diffraction or interference .Formulation of the transport equation assumes that each scattering particle is sufficiently distant from its neighbors to prevent interactions between successive scattering effects. In theory, these scatterers and absorbers must be uniformly distributed throughout the medium. Calculations of light distribution based on the radiative transport equation require knowledge of the absorption and scattering coefficients , and the phase function .Yet, to arrive at these parameters ,one must first have a solution of the radiative transport equation .Because of the difficulty of solving the transport equation exactly ,several approximation are generally used.

1.3.2 RTE in diffuse media

Scattering by a single localized scattering center is called single scattering. However in real-world systems the scattering centers are usually grouped together and the radiation is scattered more than once. This is called multiple scattering. Multiple scattering events cause the incoming radiation to be directionally randomized on interaction with the media. This light which has lost its initial directional properties due to multiple scattering events is called diffuse light. In the

diffusive transport regime where scattering dominates over absorption ($\mu_s >> \mu_a$) the light photon undergoes multiple scattering events before either being absorbed or exiting the media.

By the nature of RTE, every single absorption and scattering event that takes place in the media is considered in the Equation (1.6). In diffuse media where a photon will undergo multiple scattering events before being absorbed or exiting the media, it becomes very tedious and complex to understand each of the interactions. Although the RTE is theoretically complete, extracting meaningful solutions in such diffuse systems becomes computationally very intensive due to anisotropic multiple scattering events. To simplify this, these multiple scattering events are captured by the reduced scattering coefficient $\mu_S^{'}$ which is the inverse of the path length required for the complete randomization of the photon direction and is defined as

$$\mu_S^{'} = \mu_S(1-g) \tag{1.7}$$

where g is the anisotropy factor defined as.

$$g = \int p(\theta(\cos(\theta) d\hat{s}' \tag{1.8}$$

g takes value from -1 to 1 .If the scattering is completely isotropic g will be equal to zero as p is equal for all angles. As the particle size increases, however, the intensity distribution increases in the forward direction and p for small angles is much higher than for all other angles. Therefore, the mean cosine tends towards a value of unity, the higher the g value the more forward –peaked the scattering.

1.3.3 Kubelka-Munk Theory

Another approach to studying light transport in highly scattering media is the Kubelka-Munk theory [1.2]. Let us assume a media which is completely homogenous; a plane layer of finite thickness but infinite width and length. This is illuminated by a perfectly diffuse or collimated and homogenous source of light. KM theory assumes that the radiation passing through the medium can be divided into two “diffuse fluxes” traveling in the forward and backward directions denoted as I and J, respectively Figure 1.1. The backscattering and absorption

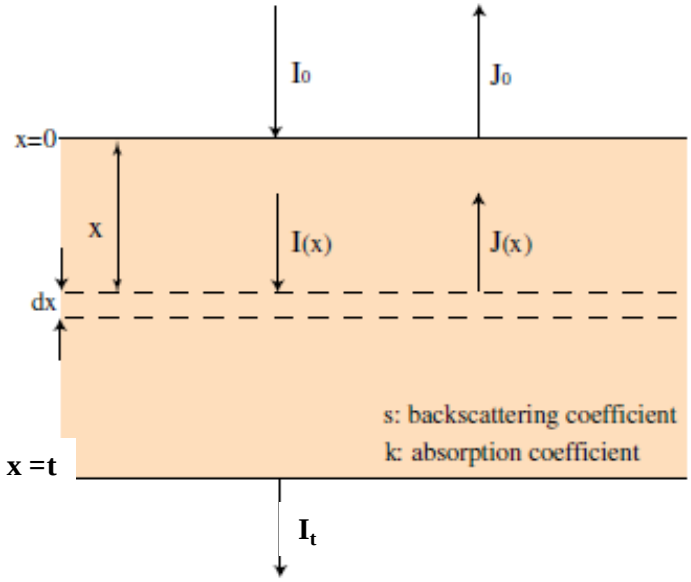

Figure 1.1. Shematic representation of light transport in a turbid medium modeled using the Kubelka-Munk (K-M) theory. *I* and *J* depict diffuse fluxes traveling in the forward and backward directions, respectively. *S* and *K* are the K-M backscattering and absorption coefficients of the medium respectively. Sample thickness is denoted by *t*.

coefficients for these diffuse fluxes (denoted as S and K, respectively) are defined by two differential equations

$$I(x+dx) = (K+S).I + S.J + I(x) \tag{1.9a}$$

$$J(x) = -(K+S).J + S.I + J(x+dx) \tag{1.9b}$$

On integrating these equations over the complete thickness'd' of the media and applying boundary conditions The reflectance and transmittance of a diffusive media of thickness t is given by

$$R = \frac{\left(1-\beta^2\right)\left(\exp(\alpha t)-\exp(-\alpha t)\right)}{(1+\beta)^2\exp(\alpha t)-(1-\beta)^2\exp(-\alpha t)}$$
$$T = \frac{4\beta}{(1+\beta)^2\exp(\alpha t)-(1-\beta)^2\exp(-\alpha t)} \tag{1.10}$$

Where $\alpha = \sqrt{K(K+2S)}$, $\beta = \sqrt{K/(K+2S)}$ and K and S are the K-M absorption and scattering coefficients respectively.

K-M coefficients are only phenomenological approximations because the theory assumes incident radiation is diffuse and the scattering is isotropic. Similar to other diffusion approximation based models, K-M theory also assumes higher scattering compared to absorption. Though these conditions are not completely met in many of the real systems, the theory nonetheless provides a simple quantitative way of describing light transport in diffused medium.In this thesis we have used K-M theory based models to extract optical parameters of a multilayered optical system.

Chapter 2

RELATION BETWEEN KUBELKA-MUNK AND RADIATIVE TRANSFER EQUATION COEFFICIENTS

The K-M coefficients introduced in Equation (1.9) are only phenomenological parameters and are not the same as the more fundamental absorption (μ_a) and scattering coefficient (μ_s) of radiative transfer equations (RTE). Though the K-M theory is a computationally simple theory, its significance is lost if the coefficients are not related to the more fundamental properties of the medium. Many authors [2.1-2.3] have derived relations between the K-M coefficients and the more fundamental radiative transfer coefficients (μ_a, μ_s and g). Here μ_a is the absorption coefficient, μ_s is the scattering coefficient and g is the anisotropy factor of the diffusive medium. In the diffusive approximation regime ($\mu_s >> \mu_a$), the general form of the relations between the K-M coefficients and the radiative transfer coefficients derived by different authors can be written as

$$\begin{aligned} S &= x\mu_s' - y\mu_a \\ K &= z\mu_a \end{aligned} \tag{2.1}$$

where, $\mu_s' = \mu_s (1-g)$ is the reduced scattering coefficient. For an isotropic medium, Klier [2.1] had shown $\mu_a = \eta K$ and $\mu_s = \chi S$ with the value of η varying from 0.5 to 1 while the value of χ varying from 4/3 to 3.33. van Gemert and Star [2.2] extended this further to show that the K-M coefficients can be related to the reduced scattering coefficient in an anisotropic medium. For an anisotropic and highly scattering medium, they showed $K=2\mu_a$ and $S = (3\mu_s (1-g)-\mu_a)/4$. However, in most of the measurement geometries, the condition that the incident beam is diffusive is not met. It is either fully collimated or partly collimated and partly diffusive. Various authors have extended this model further to include collimated incident flux and have shown that the K-M theory is also applicable in the case of collimated beam [2.4-2.6]. Thennadil [2.6] has shown that, for a collimated incident beam in the high scattering regime, S depends only on scattering, however the relation should be modified to include a function dependent on the anisotropy factor, $S=12\mu_s'/(4.8446+.472g-.114g^2)^2$.

Recently, Roy et al [2.7] have developed simple empirical relations to relate the K-M coefficients to the absorption μ_a and reduced scattering μ_s' coefficients of the radiative transfer equation. Reduced scattering coefficient is the effective scattering of a collection of particles due to multiple scattering and is defined as $\mu_s' = (1-g)\ \mu_s$ where μ_s and g are the scattering coefficient and anisotropy factor of the individual particles respectively. The method used by them to obtain the empirical relations is shown schematically in Figure 2.1.

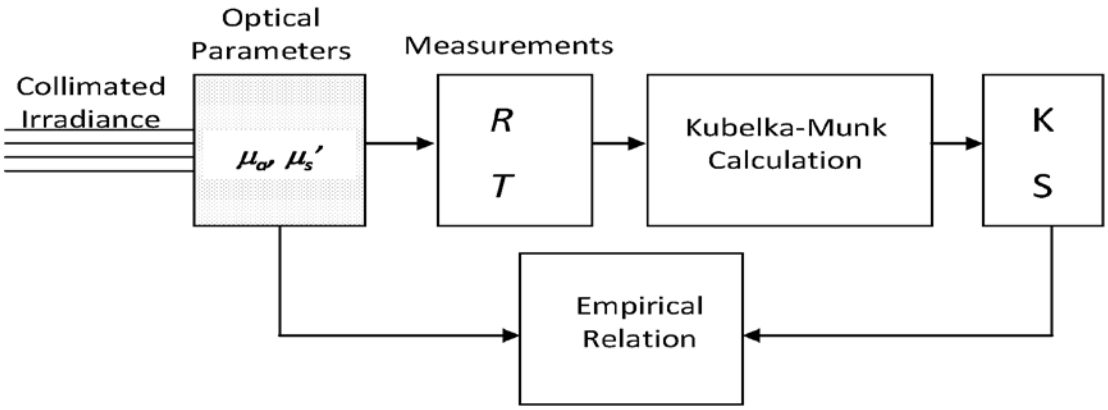

Figure 2. 1. Schematic diagram of the method used to obtain empirical relations between radiative transport coefficients and the Kubelka-Munk coefficients. From the measured total reflectance (R) and transmittance (T), the K-M coefficients were calculated and related. This method was borrowed from the work of Roy et al [2.7].

They prepared turbid samples with known scattering properties and absorption properties (μ_a and μ_s') using a mixture of mono dispersed polystyrene spheres and a colored dye with known absorption properties. For samples with different values of (μ_a and μ_s'), they measured the total transmittance T (both collimated and diffuse) and total reflectance R. Using the measured values of T and R, they solved Equation (1.10) to obtain the corresponding K-M coefficient K and S. Finally, they obtained empirical relationships between the calculated sets of K and S values and the sets of radiative transfer coefficients (μ_a and μ_s') used in the turbid samples. They have shown that the K-M coefficients can be related to μ_a and μ_s' by the following relation:

$$S = a\ \mu_s'$$
$$K = \mu_a + b\ (\mu_a \mu_s')^c \qquad (2.2)$$

where *a*, *b* and *c* are constants. These empirical relations were capable of predicting the concentration of chromophores within an error of 10%.

In this thesis, we have modified Roy et al's empirical relation to improve accuracy and used the modified relations to decouple scattering and absorption properties of turbid samples. In this chapter we describe the method used to obtain the more accurate relations and validation of the empirical relation in extracting the absorption and reduced scattering coefficients of a turbid medium.

2.1 Material and Methods

2.1.1 Sample Preparation

In order to obtain the parameters in the empirical relations, two types of samples were prepared. First set of turbid samples, which were purely scattering, were prepared using different concentrations of one micron polystyrene microspheres. The polystyrene microsphere dispersion was obtained from Duke Scientific, USA. From a stock solution containing approximately 2 wt% of 1 micron diameter polystyrene microspheres, five samples were prepared with 200 μl, 100 μl, 50 μl, 25 μl and 12.5 μl of stock solution in 1 ml of milliQ water each. The reduced scattering coefficient of the samples varied from 0.06 mm^{-1} to 1.4 mm^{-1} in the 450 – 650 nm range. Second set of samples, which were absorbing and scattering, were prepared by mixing known amounts

Table 2. 1 Samples with different concentration of dye and polystyrene microspheres used to obtain empirical relation shown in equation 2.4.

Sample	Dye concentration	Polystyrene concentration
Sample 1	9 ppb	56 μl/ml
Sample 2	9 ppb	112 μl/ml
Sample 3	20 ppb	50 μl/ml
Sample 4	20 ppb	100 μl/ml

of Allura Red dye (CI 16035) and the polystyrene microspheres. The Allura Red dye was obtained from Roha Dyechem Pvt Ltd., India. Four samples were prepared by combining

different concentration of dye and polystyrene microsphere as shown in table 2.1. The absorption coefficient of the dye varied from 0 to 0.2 mm^{-1} in the measurement range of 450 – 650 nm. For validation of the empirical relations, a sample containing a mixture of 20ppb of dye and 100 µl/ml of polystyrene microspheres were used.

2.1.2 Spectral Measurements

A Perkin Elmer Lamda 900 UV-Vis spectrophotometer was used to (i) measure absorption spectra of the dye and (ii) the extinction spectra of the polystyrene spheres. Total reflectance *R* (diffuse and specular) of the samples was measured using a portable spectrophotometer (Model 2600d, Konica Minolta, Japan.) comprising of a pulsed Xenon lamp and a 52 mm integrating sphere.. The configuration used in the reflectance measurement is shown in Figure 2.2a. The sample was illuminated through 8mm diameter aperture and the reflected light is collected through 8 degree viewing angle and is analyzed using a holographic grating and a photodiode array. The reflectance was measured in the wavelength range of 450 nm to 650 nm with a spectral resolution of 10 nm. The reflectance values were measured relative to a Spectralon® reflectance standard with a reflectance value of 99% in the 450-650 nm range.

Full spectrum total transmittance *T* (collimated and diffuse) of the samples were measured using a system which included a LED light source (Brite Lite, USA), a 90 mm diameter integrating sphere (Labsphere, USA) and a spectrometer (ILT 900 from International light, USA). The configuration used in this measurement is shown in Figure 2.2b. A water filled cuvette was used as reference during transmittance measurements in order to account for reflectance losses from

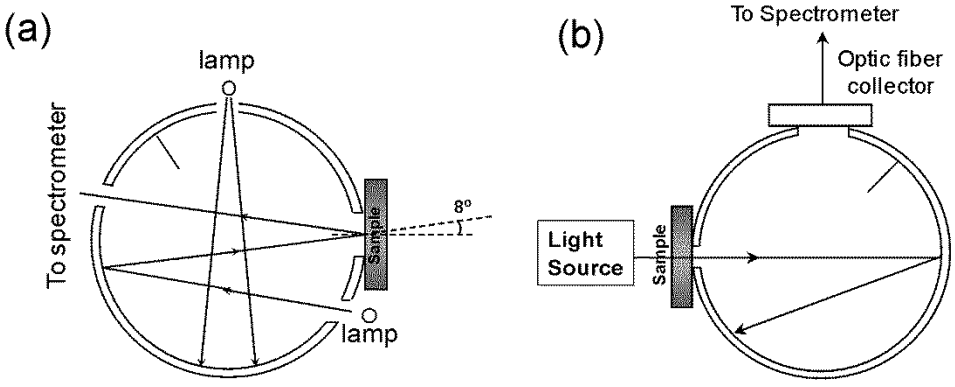

Figure 2.2. Measurement configuration used to measure (a) Total reflectance and (b) Total transmittance.

the cuvette walls. To take into account transmittance measurement errors resulting from the differing reflectance properties of the sample and reference, dual port geometry was used. During reference measurement, the reference cuvette was placed at the entry port and the sample cuvette was placed at the dummy port of the integrating sphere. During the sample measurement, their positions were interchanged. For both *T* and *R* measurements, two thin cuvets (660 microns and 750 microns thick) were used in order to avoid loss of light in the lateral directions.

2.1.3 Calculation of absorption and reduced scattering coefficients

The scattering coefficient (μ_s) of the polystyrene spheres was calculated from the measured extinction (*E*) using the relation $\mu_s = 2.302\ E$ cm^{-1}. A factor of 2.302 was used to convert the common logarithm (log) to natural logarithm (ln). The anisotropy factor *g* was calculated using a Mie scattering calculator developed by Philip Laven [2.8]. The reduced scattering coefficient was calculated using the relation $\mu_s' = \mu_s (1-g)$. In order to decouple the absorption and reduced scattering coefficients of the samples, the K-M coefficients were first calculated using Equation (1.10) using measured *R* and *T*. From the K and S values, μ_a and μ_s' were calculated using the empirical relation obtained in the next section and shown in Equation (2.5).

2.2 Results and Discussion

2.2.1 Derivation of Empirical Relation between K-M and RTE coefficients

In order to obtain the relation between μ_s' and the K-M scattering coefficient *S*, the total reflectance *R* and total transmittance *T* of the five purely scattering polystyrene solutions were measured in the wavelength range of 450-650 nm. Using Equation (1.10), the S values were calculated at different wavelengths for the 5 different concentrations. Using the method described in the materials and methods section, the reduced scattering coefficients of the 5 samples were calculated for the entire measurement range of 450-700 nm. In Figure 2.3, *S* values of the five samples are plotted as a function of reduced scattering coefficient (μ_s') for all wavelengths. Different cluster of points in Figure 2.3 corresponds to five different samples and the different points in the clusters correspond to different wavelengths. From Figure 2.3, it is clear that the *S* depends linearly on μ_s' as described by Thennadil [2.6] and Gates [2.9]. Best fit

between S and μ_s' is obtained for a slope of 0.59. Hence the relation between S and μ_s' in Equation (2.2) can be written as

$$S = 0.59\ \mu_s^{'} \tag{2.3}$$

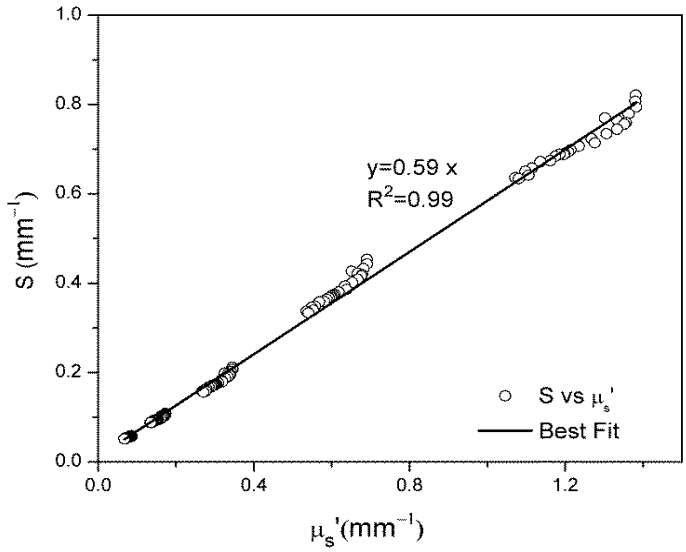

Figure 2. 3. K-M scattering coefficient S as a function of reduced scattering coefficient μs' of the polystyrene microspheres. Each cluster of points corresponds to different concentration of polystyrene spheres and different points in a cluster correspond to different wavelengths. The solid line is the best linear fit obtained.

Roy et al [2.7] used the empirical relation shown in Equation (2.3) to relate *K* to μ_a and μ_s'. In Equation (2.2) for K, the second term can be attributed to the additional absorption due to increased path length resulting from multiple scattering. They used an empirical relation $b\left(\mu_a \mu_d^{'}\right)^c$ to describe the additional absorption. Since absorption and scattering are two independent properties, the power law dependence of additional absorption term need not be the same for both absorption and scattering. Instead of the relation shown in Equation (2.2), the following relation with two independent powers for absorbance and scattering are used here.

$$K = \mu_a + \left(\mu_a^b \mu_s^{'c}\right) \tag{2.4}$$

To obtain the parameters b and c, the *T* and *R* values of the four turbid samples containing dye and polystyrene spheres were measured in the wavelength range 450-650 nm. From the *T* and *R*

values, the K and S values were calculated using Equation (1.10). The μ_s' values were calculated from the measured S values assuming the relation in Equation (2.3) is valid even in the presence of absorption. Since the μ_a, μ_s' and the *K* values are known, fitting the values in Equation (2.4),

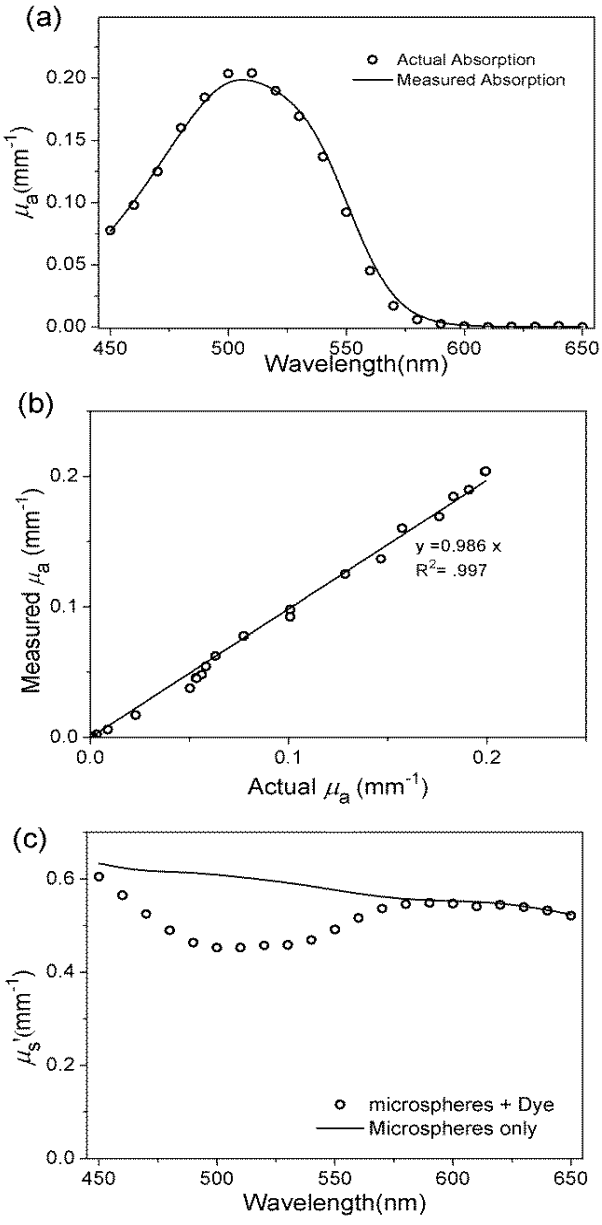

Figure 2.4. The actual (circles) and extracted (solid line) values of (a) absorption coefficient of the dye and (b) linear fit between actual and extracted absorption coefficient of the dye showing less than 2% variation, (c) reduced scattering coefficient of pure polystyrene spheres (solid line) and polystyrene spheres in the presence of dye (circles).

we find the b=0.72 while c=0.4. Now the relations in Equation (2.3) and (2.4) can be written as

$$S = 0.59\ \mu_s^{'}$$
$$K = \mu_a + (\mu_a^{0.72}\mu_s^{'0.4}) \tag{2.5}$$

2.2.2 Validation of the empirical equation

In order to validate the empirical relation, the R and T values of the turbid sample with known absorption and scattering properties were measured. The K and S values were calculated from the measured R and T values using Equation (1.10). Using the empirical relation shown in Equation (2.5), μ_a and μ_s' values were calculated from the K and S values. In Figure 2.4a and Figure 2.4c, we have shown the μ_a and μ_s' values of the pure dye and pure polystyrene particles along with the extracted values of μ_a and μ_s' using the empirical relation in Equation (2.5). In Figure 2.4b, we have plotted the linear fit between actual and extracted values of absorption coefficient. Linear fit with a slope of 0.985 indicates that average error in measurement is less than 2% indicating that this method can be used to extract absorption coefficient of turbid samples accurately from the measure T and R values. We find that the μ_s' values of polystyrene spheres in the presence of absorption vary from the pure polystyrene value. At wavelengths where the absorption is high, the scattering decreases. At higher μ_a, the imaginary refractive index of the surrounding medium increases leading to higher drop in the scattering value. In the next section we derive an empirical relation to calculate the pure scattering properties of the scatterers in the absence of absorbance from their reduced scattering value in the presence of absorbing materials.

Chapter 3

EMPIRICAL RELATION BETWEEN REDUCED SCATTERING COEFFICIETNS IN THE ABSENCE AND PRESENCE OF ABSORBING MEDIUM

In the previous section, empirical relations between the K-M and RTE coefficients were derived. Though the empirical relations are capable of extracting the absorption coefficient of the turbid medium, it was found that the reducing scattering coefficients of the scatterers decrease in the presence of absorbing medium. Various authors [3.1-3.3] have discussed the dependence of scattering on absorbance of the surrounding media and shown that the scattering decreases due to the absorbance of the surrounding media. In this section, we will discuss derivation of an empirical relation between the reduced scattering coefficient in the absence of absorption $\mu_s'(0)$ and reduced scattering coefficient in the presence of absorption $\mu_s'(\mu_a)$. This will help us determine the pure scattering properties of the scatters in the turbid medium.

3.1 Materials and Methods

In order to derive an empirical relation between the reduced scattering coefficients in the absence and presence of absorbing materials, four different turbid samples were prepared with each containing 100 μl of approximately 2% polystyrene dispersion in 1 ml of milli Q water. While the first sample contained no dye, the other three samples contained 10 ppm, 20 ppm and 30 ppm of the dye respectively. As in the previous section, the total reflectance *R* and total transmittance *T* of the samples were measured.

3.2 Results

From the measured *R* and *T* values, *K* and *S* values were calculated using the Equation (1.10). Then from the *K* and *S* values, μ_a and μ_s' values of all four samples were calculated using the empirical Equation (2.5). The extracted μ_a values are plotted in Figure 3.1a. In Figure 3.1b, we have plotted the extracted reduced scattering values μ_s' of pure polystyrene spheres along with the reduced scattering values of polystyrene spheres in the presence of different concentrations

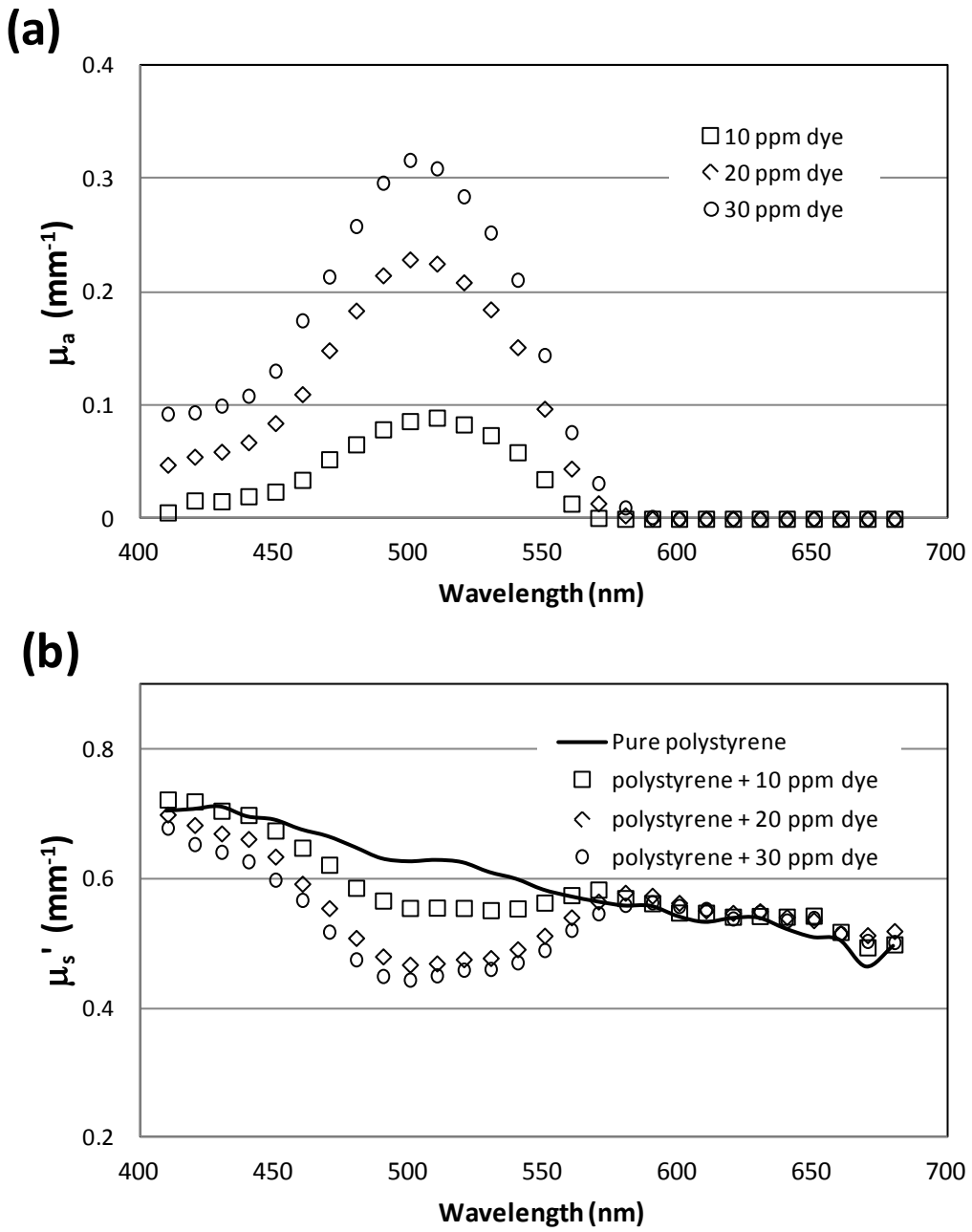

Figure 3. 1. The absorption coefficient of a polystyrene spheres and dye mix extracted using the empirical equation 2.5 for three different dye concetrations. (b). The reduced scattering coefficients of the pure polystyrene sand polystyrene-dye mix with three different dye concetrations extracted using equation 2.5.

of dye. It is clear that the reduced scattering coefficient values decreases in the presence of absorption. As the absorption decreases, the deviation from the pure polystyrene value increases.

3.3 Development of empirical relation between reducing scattering coefficients in the presence and absence of absorbing medium

Reduced scattering represents the collective, isotropic scattering of a large number of scattering events. In reduced scattering, multiple scattering events are replaced with a "single" effective isotropic scattering event which is generally "reduced" compared to the single scattering events. The length scale of reduced scattering is generally larger than the single scattering events. Hence the light scattered in these length scale travel large distances and part of the light will be absorbed by the surrounding medium. In order to derive the empirical relation we start with the following extreme conditions. When the absorbance is zero, the reduced scattering should be equivalent to that of the pure scatterer. When the absorbance is very large μ_a >>1, scattering should be negligible since the absorbance will dominate the transport. For small values of μ_a, the scattering should decrease from the values of pure scatterer. One function which obeys all these conditions is the exponential decay function. We propose that the empirical relation should have the following form

$$\mu_s'(\mu_a) = \mu_s'(0) \exp(-a*\mu_a) \tag{3.1}$$

where $\mu_s'(0)$ is the reduced scattering coefficient of the pure scatterer in the absence of

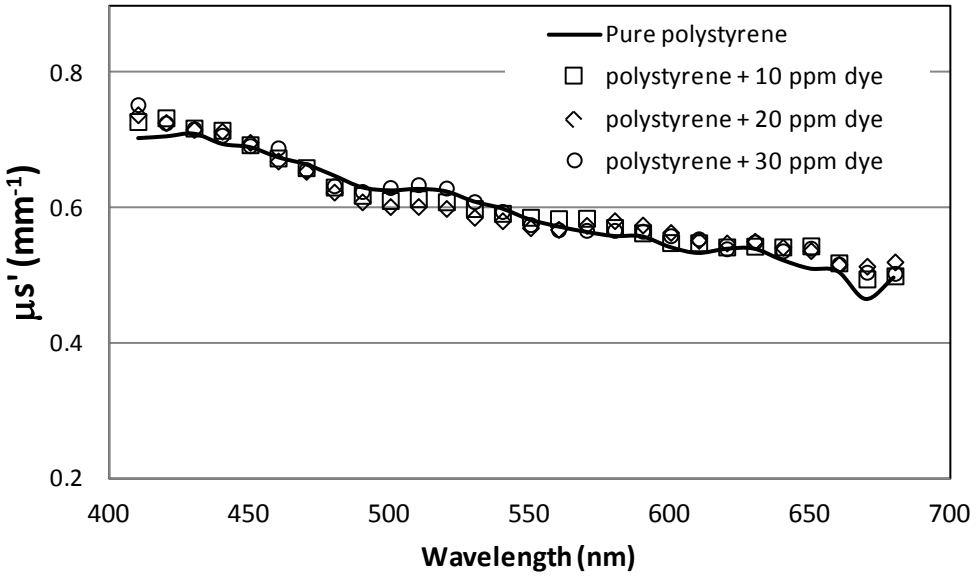

Figure 3. 2. The reduced scattering coefficient of a polystyrene spheres extracted using the empirical relation shown in equation 3.2 plotted along with the reduced scattering coefficient of the pure polystyrene spheres.

absorbing medium, $\mu_s'(\mu_a)$ is the reduced scattering coefficient of the scatterers in the presence of absorbing medium and a is the fitting parameter. By varying the parameter a, we have fitted the data shown in Figure 3.1b to the pure scattering values of the polystyrene spheres. For a =1.1, we obtain the best fit as shown in Figure 3.2.

With a=1.1, the above relation simply becomes

$$\mu_s'(\mu_a) = \mu_s'(0) \exp(-1.1\mu_a) \tag{3.2}$$

Inverting the relation, the reduced scattering coefficient of the scatterer in the absence of absorption can be derived from the reduced scattering coefficient in the presence of absorbance.

$$\mu_s'(0) = \mu_s'(\mu_a) \exp(1.1\ \mu_a) \tag{3.3}$$

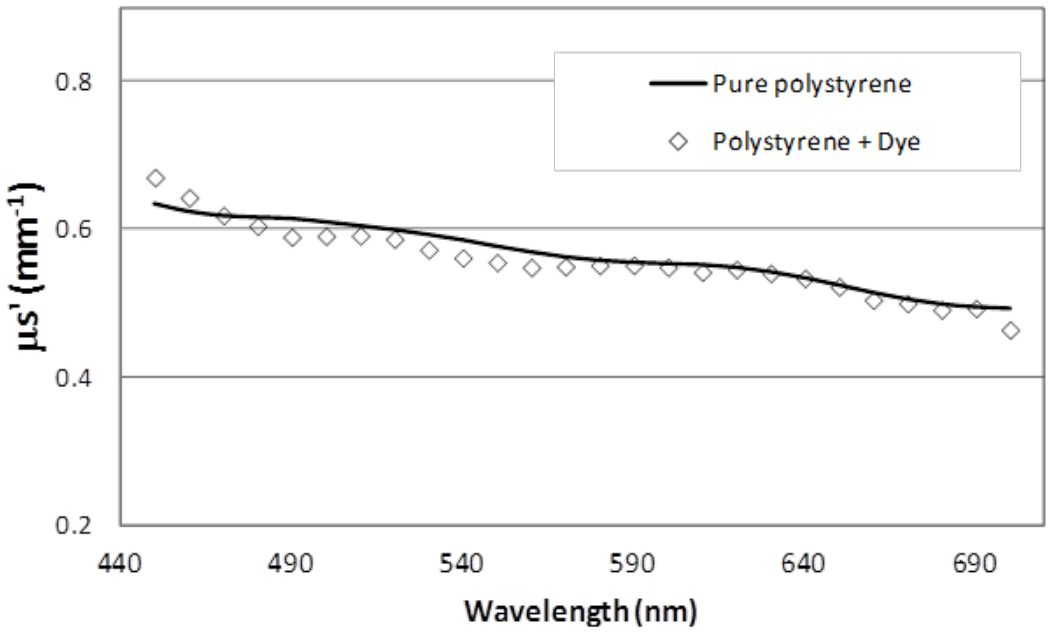

Figure 3. 3. The reduced scattering coefficient of polystyrene spheres (diamonds) was extracted from the reduced scattering coefficient of the polystyrene and dye mix using equation 3.3. The reduced scattering coefficient of pure polystyrene spheres is also shown(solid line). This data is same as the data shown in figure 2.3 c.

Now using the above relation, we determine the reduced scattering of the pure polystyrene particles from the reduced scattering of the polystyrene in the presence of dye shown in Figure 2.4c. This $\mu_s'(0)$ obtained using Equation(3.3) matches very well with the $\mu_s'(0)$ measured for

the pure polystyrene sphere and is shown in Figure 3.3. This indicates that not only we can extract the absorption properties of the turbid using Equation (2.5), we can also derive the pure scattering properties of the medium using Equation (2.5) and Equation (3.3).

Chapter 4

DEVELOPMENT OF A DOUBLE LAYER TURBID MEDIA MODEL

Since the K-M theory provides the analytical expression of both transmittance and reflectance of the diffusive layers, it can be extended to describe the multilayered structures also. When coupled with the empirical relations derived in chapter 3 and chapter 4, this becomes a very powerful, but simple way of extracting the optical parameters of multilayered materials. There are many multilayered materials which of interest in nature. Examples of multi layer materials include epithelial layers in tissues, skin and plant structures such as leafs. A multilayer model coupled with the transmittance and reflectance measurement can be used to non-invasively extract optical parameters of various multilayer systems.

4.1 Materials and Methods

4.1.1 Theory

Many authors have developed multi-layer models to describe reflection from inhomogeneous turbid samples [4.1-4.4]. Since the K-M theory provides analytical expression of both transmittance and reflectance of the individual layers, it can be extended to describe multi-layered structures also. If R_1, R_2…,R_n and T_1, T_2…T_n are the reflectance and transmittance of the different layers which can be calculated using Equation (1.10) and the empirical relations shown in Equations (2.5) , then the total reflectance and transmittance of the layers can be calculated in the following way. If I_n is the light flux travelling in the forward direction and J_n is the light travelling in the reverse direction from the nth layer respectively, then we can write:

$$\begin{aligned} I_1 &= I_0T_1 + J_1R_1 \; and \; J_0 = J_1T_1 + I_0R_1 \\ I_2 &= I_1T_2 + J_2R_2 \; and \; J_1 = J_2T_2 + I_1R_2 \\ &\vdots \\ I_n &= I_{n-1}T_n + J_nR_n \; and \; J_{n-1} = J_nT_n + I_{n-1}R_n \end{aligned} \tag{4.1}$$

The total reflectance $R=J_0$ and total transmittance $T=I_n$. With $I_0=1$ and $J_n=0$ as boundary conditions, these Equations can be solved self consistently to obtain the values of $R=J_0$. For example, for a two layer structure shown in Figure 4.1, solving Equation (4.1) self consistently results in the following relation:

$$R = R_1 + \frac{T_1^2}{1 - R_1 R_2} \quad and \quad T = \frac{T_1 T_2}{1 - R_1 R_2} \tag{4.2}$$

4.1.2 Optical Phantoms

In order to validate the double layer shown in Equation (4.2) and validate the feasibility of extracting optical parameters of double layers using the empirical relations shown in Equation (2.5) and Equation (3.3), we fabricated optical phantoms with known optical parameters. The optical phantoms were made by dispersing known concentrations of iron oxide particles in Sylgard^{TM} in a cuvet made of two parallel glass plates. The dispersion was cured in an oven for about 2 hours at a temperature of 60 degrees C. The optical phantoms thus obtained are shown in Figure 4.1. Two such phantoms were made with 1.65 mg/ml and 2.5 mg/ml of iron oxide

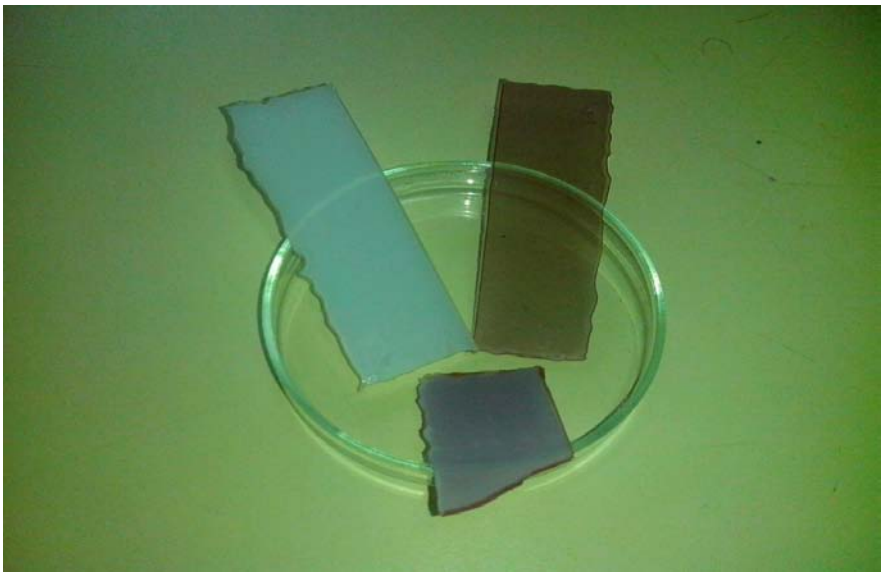

Figure 4. 1. Images of optical phantoms used in the multi-layer model study

respectively.

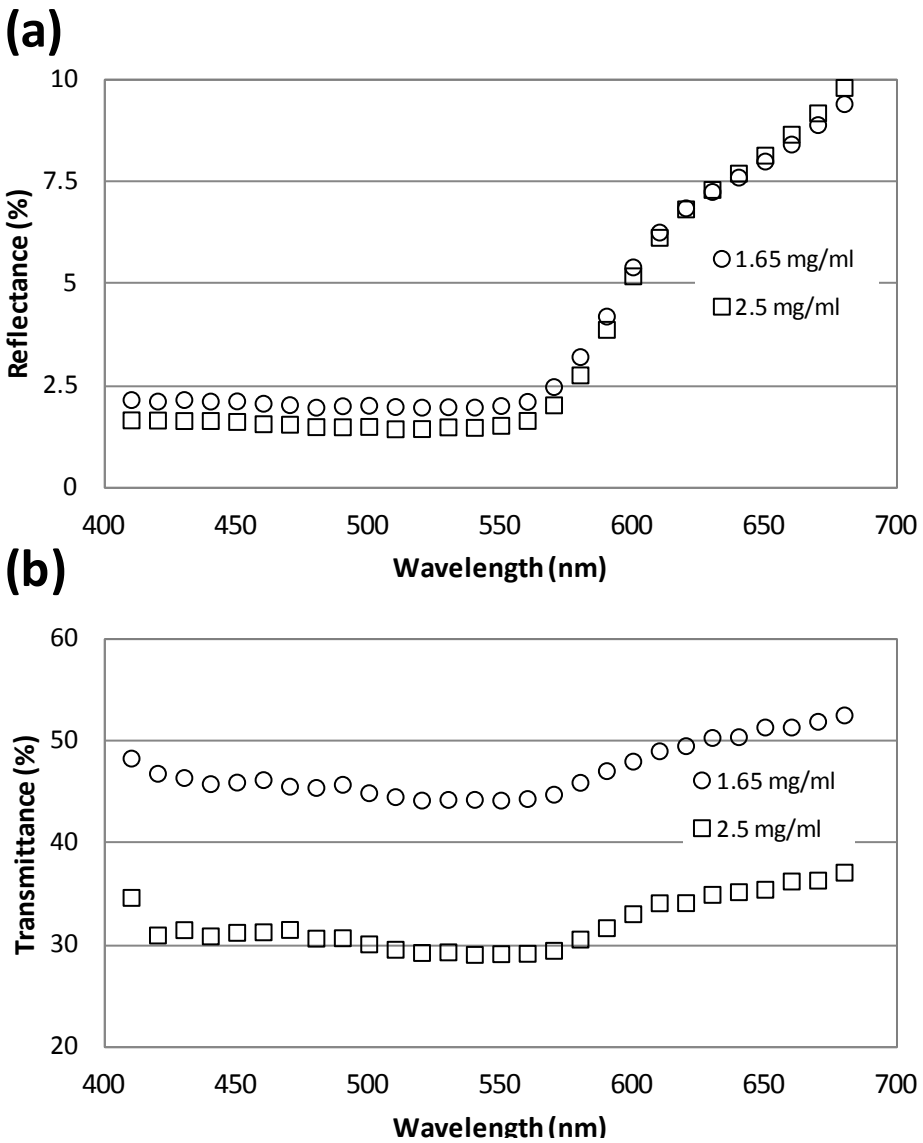

Figure 4.2. (a) Reflectance and (b) transmittance values of the two individual tissue phantoms

4.2 Results and Discussion

The transmittance and reflectance values of the two layers were measured as described in the previous sections. The reflectance and transmittance values of the individual iron oxide layers are shown in Figure 4.2a and Figure 4.2b respectively. From the measured transmittance and reflectance values, the optical properties namely the specific absorption coefficient and specific reduced scattering coefficient of the layers were extracted using the Equations (1.10), (2.5) and (3.3). These values are shown in Figure 4.3.

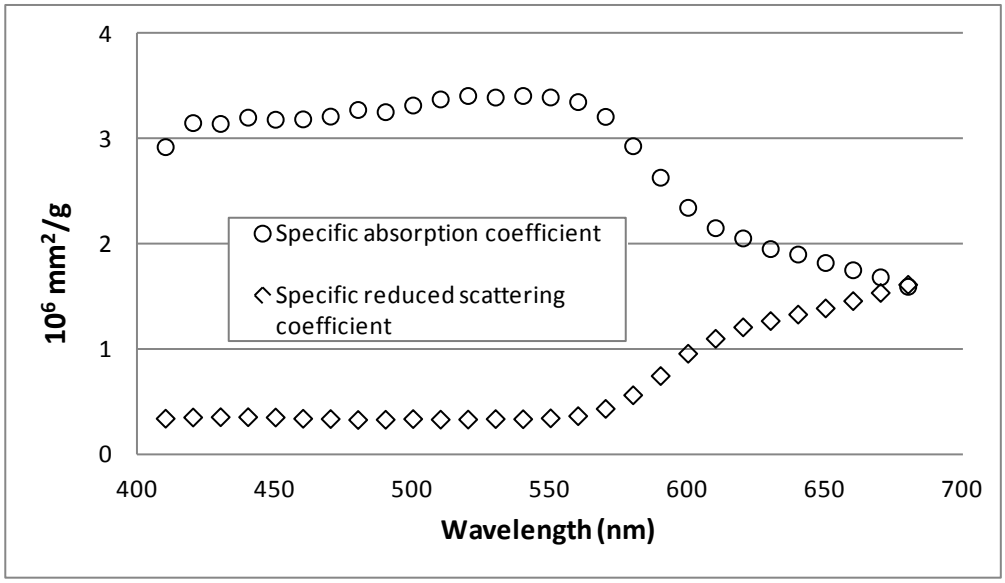

Figure 4.3. The specific absorption and specific reduced scattering coefficients of the iron oxide used in the optical phantoms, calculated using the empirical relation shown in equation 2.5

In order to validate the two layer model, and feasibility using the two layer model in extracting the optical parameters of these two layers, we combined the two iron oxide optical phantoms and measured its reflectance at different wavelengths which are shown in Figure 4.4 (solid squares). In order to extract the optical parameters namely the concentration of iron oxide and thickness of the two layers, we followed the following procedure.

- Four parameters namely the concentrations of iron oxide in the two layers and thicknesses of the two layers were used as variable parameters.
- By multiplying the specific absorption and specific reduced coefficients shown in Figure 4.3 by the variable concentrations of the two layers, the absorption and reduced scattering coefficients of the two layers were calculated.
- Using the absorption and reduced coefficients and the two variable thickness parameters, the reflectance and transmittance of the two layers were calculated using Equation (1.10) and Equation (2.5).
- With calculated reflectance and transmittance layers of the individual layers, the reflectance of the combined double layer was calculated using Equation (4.2).

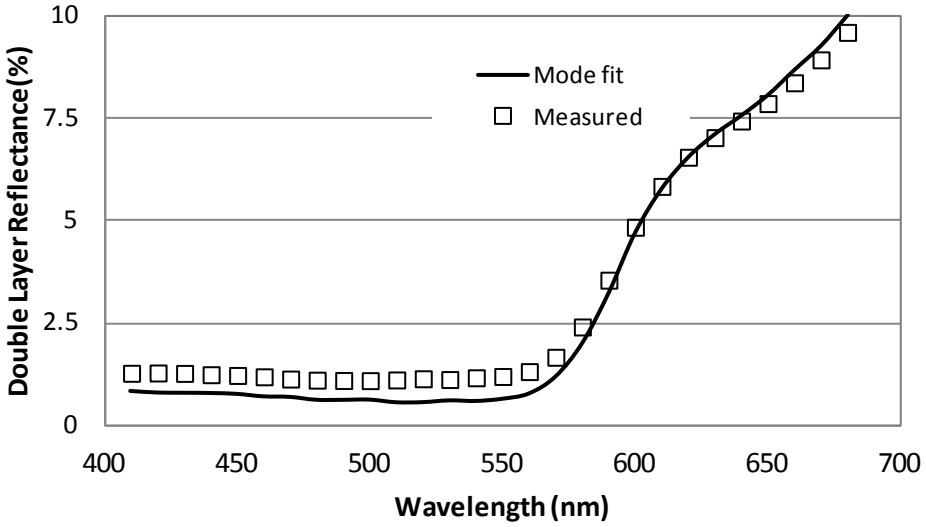

Figure 4. 4. The measured reflectance (solid line) of the double layer skin phantom plotted along with double layer model fitting. The concentrations of iron oxide and thickness of the two layers were used as fitting parameters to obtain the best fit.

- The difference between the measured double layer reflectance shown in Figure 4.4 (squares) and the reflectance of the double layer calculated using the above procedure was minimized by varying the two concentration and two thickness parameters.

The best fit thus obtained for the combined reflectance of the double layer is shown in Figure 4.4 (line) and parameters used to obtain the best fit are shown in table 4.1 along with the actual concentration and thickness of the two layers. From the Figure 4.4, it is clear that we get a good fit between the measured and calculated reflectance.

Table 4.1. The extracted optical parameters of the double layer optical phantom along with the actual values

Parameters	Extracted Value	Actual Value
Iron oxide concentration – first layer	1.5 mg/ml	1.65 mg/ml
Iron oxide concentration – second layer	2.65 mg/ml	2.5 mg/ml
First layer thickness	1 mm	1.1 mm
Second layer thickness	1 mm	1.1 mm

From table 4.1, it is clear that the fitting parameters match very well with the actual values of concentration and thickness. The difference between the extracted and actual parameters is less than 15% establishing the feasibility that our method is capable of extracting the optical parameters of double layer systems.

Chapter 5

CONCLUSION

One of the key challenges in strongly scattering media is to decouple absorption from scattering. Various authors have tried to use diffuse optical spectroscopy to address this. However these measurements involve computer intensive calculations to obtain optical parameters from the diffuse optical spectra. Kubelka-Munk (K-M) theory is a phenomenological light transport theory that provides analytical expressions for reflectance and transmittance of diffusive substrates. Many authors have derived relations between coefficients of K-M theory and that of the more fundamental radiative transfer Equations (RTE). In this thesis, we have modified an empirical model developed earlier by Roy et al [2.7] to relate the K-M and RTE coefficients and improved its accuracy.

We have validated the feasibility of using these empirical relations to decouple the absorption and scattering properties of a turbid medium. We find that in presence of absorption, the scattering properties of a scattering material decreases. We have developed an empirical Equation to obtain the reduced scattering coefficient of the pure scattering material from the scattering properties of the same material in the presence of absorption which can predict the reduced scattering coefficient very accurately.

Many materials observed in nature exhibit multilayer optical structures. Few examples include skin of humans, epithelial cells, leaf in plants etc. The optical properties of these materials are of great interest to scientists for variety of reasons including disease diagnosis, chlorophyll estimation etc. We have built a double layer optical model using the K-M theory. In order to validate the model we developed optical phantoms using a mix of PDMS and commercially available iron oxide particles. Using the empirical relations and the double layer model we can extract the optical properties of the double layer optical phantom system within an error of 10% establishing the feasibility that this model can be used to study the optical properties real systems such as skin tissues and plant leafs.

REFERENCES

1.1. H. C. Van de Hulst, Light scattering by small particles (Dover Publications, 1981).

1.2. P. Kubelka and F. Munk, “Ein Beitrag zur Optik der Farbanstriche,” Zeits. f. tech. Physik 12, 593–601 (1931).

1.3. A.Ishimaru, Wave propagation and scattering in Random media, Vol. 1,Academic press, New York,1978 .

1.4. K.M.Case and P.F.Zweifel, Linear Transport Theory Addison-Wesley ,Reading ,PA,1967.

2.1. K. Klier, “Absorption and scattering in plane parallel turbid media,” J. Opt. Soc. Am., 62, 882-885 (1972).

2.2. M. J. C. van Gemert and W. M. Star, “Relations between the Kubelka-Munk and transport equation models for anisotropic scattering”, Lasers Life Sci., 1, 287-298 (1987).

2.3. B. J. Brinkworth, “Interpretation of the Kubelka-Munk coefficients in reflection theory,” Appl. Opt. 11, 1434-1435 (1972).

2.4. J. T. Atkins, Absorption and scattering of light in turbid media, Ph. D. Dissertation, University of Delaware, 1965.

2.5. J. Reichman, Determination of absorption and scattering coefficients for non-homogeneous media. 1: Theory., Appl. Optics, 12, 1811-15 (1973).

2.6. S. N. Thennadil, “Relationship between the Kubelka–Munk scattering and radiative transfer coefficients,” J. Opt. Soc. Amer. A., **25,** 1480-1485 (2008).

2.7. A. Roy, R. Ramasubramaniam, and H. A. Gaonkar, “Empirical relationship between Kubelka–Munk and radiative transfer coefficients for extracting optical parameters of tissues in diffusive and nondiffusive regimes,” J. Biomed. Optics **17**, 115006 (2012).

2.8. http://www.philiplaven.com/mieplot.htm

2.9. L. F. Gates, “Comparison of the photon diffusion model and Kubelka–Munk equation with the exact solution of the radiative transport equation,” Appl. Opt. **13**, 236–238 (1974).

3.1. J. Reichman, “Determination of absorption and scattering coefficients for non-homogeneous media. 1: theory,” Appl. Opt. **12**, 1811–1815 (1973).

3.2. . J. Yin and L. Pilon, “Efficiency factors and radiation characteristics of spherical scatterers in an absorbing medium,” J. Opt. Soc. Am. A **23**, 2784-2796 (2006).

3.3. Q. Fu and W. Sun, “Mie Theory for Light Scattering by a Spherical Particle in an Absorbing Medium,” *Appl. Opt*. **40**, 1354-1361 (2001).

4.1. Anderson R. R and J. A. Parish, The optics of human skin, J. Invest. Derm. **77**,13 (1981)

4.2. Zonios G, J Bykowski and N Kollias, Skin melanin, hemoglobin and light scattering properties can be quantitavely assessed in-vivo using diffused reflectance spectroscopy, J. Invest. Derm. **117**,1452 (2001)

4.3. Neilsen K P, L Zhao, P Juzenas, J J Stamnes, K Stamnes and J Moan, Reflectance spectra of pigmented and non-pigmented skin in the UV spectral region, Photochemistry and Photobiology **80**, 450 (2004)

4.4. Prahl S A, M J C Van Gemert and A J Welch, Determining the optical properties of turbid media using the adding-doubling method, Applied Optics, **32**, 559–568 (1993).